

# Optical Properties Transformation under Laser Treatment of Hybrid Organic–Inorganic Thin Films

Rasim Saifutiyarov, Olga Petrova, Ilya Taydakov, Alina Akkuzina, Artem Barkanov, Marina Zykova, Alexey Lipatiev, Vladimir Sigaev, Roman Avetisov, Vladislav Korshunov, and Igor Avetissov\*

Thin films (50–100 nm) of hybrid materials (HM's) based on inorganic matrices and organic phosphor are prepared by layer-by-layer vacuum deposition on glass substrates. The possibility of an exchange solid-phase reaction between the organometallic phosphor (tris-(8-hydroxyquinolate) aluminum) and inorganic compounds without thermal heating of the sample volume is demonstrated. The reaction is stimulated by Pharos SP laser (1030 nm wavelength, 180 fs pulse duration, 100 kHz pulse repetition rate, maximum power 6 W) with localization of the reaction region to the focused laser beam waist (diameter of  $\approx 1 \mu\text{m}$ ). The resulting products have a photoluminescence (PL) intensity exceeding the PL intensity of the original organometallic phosphor. Local modification of HM's thin films by femtosecond laser beam allows creating 2D integrated optics elements.

## 1. Introduction

Organo–inorganic hybrid materials (HM's) allow creating materials with new functional properties, which combine the variability of organic compounds with the thermodynamic stability of inorganic substances.<sup>[1–5]</sup> Bulk HM's could be fabricated by different pathways.<sup>[6–9]</sup> It was demonstrated that the melting technique allowed synthesizing luminescent HM's by the proceeding of an exchange reaction between a coordinating organometallic phosphor and an inorganic low-melting glass matrix.<sup>[10–13]</sup>

HM's based on inorganic glass matrix and metal-organic phosphors have demonstrated photoluminescence (PL) which depends on both organic and inorganic constituents.<sup>[10,12]</sup> It has been established that during the synthesis at high temperature in melted inorganic glass an exchange reaction between organic ligands and metal ions of inorganic constituent have been

proceeded.<sup>[10]</sup> Bulk HM's based on inorganic glass matrix of the composition 80(mol%)  $\text{PbF}_2$  – 20(mol%)  $\text{B}_2\text{O}_3$  and various organic phosphors complexes of 8-hydroxyquinoline with I, II, and III groups metals of the Periodic Table<sup>[10,11]</sup> and lanthanide phenanthroline complexes<sup>[12,13]</sup> has been found to show efficient PL at phosphor contents about 0.1 wt% in the matrix. Partial HM's crystallization led to PL intensity increase in 1.5–5 times.

HM thin-film structures based on tris(8-hydroxyquinoline)aluminum ( $\text{Alq}_3$ ) and  $\text{B}_2\text{O}_3$  were fabricated and an exchange chemical reaction inside the multilayer structures was initiated by localized heating by a laser beam (758 nm).<sup>[14]</sup> By controlling the laser heating, regions with different spectra and intensity of luminescence were created, forming a given pattern.

During the exchange reaction the coordinating ion of the organometallic phosphor was dissolving in a glass matrix while one of the glass matrix ions was coordinating with the organic ligands. A new phosphor was forming in the structure of the glass matrix on the molecular level. This new material is commonly called a hybrid material.

From a thermodynamic point of view, such reaction could be stimulated by changing of any intensive thermodynamic parameter: temperature,<sup>[10]</sup> laser beam action.<sup>[14,15]</sup> In the latter case, we could not say definitely which of the factors, i.e., laser-induced heating or photon energy influenced more significantly on the reaction proceeding.

Femtosecond laser treatment makes it possible to separate in time the processes of heating and photon energy impact. So, the goal of the present research was the analysis of processes of characteristics' transformation of HM's under femtosecond laser irradiation.

In previous studies, low-melting glass systems based on boron oxide with other oxide and fluoride compounds were used to lower the temperature of the exchange reactor. However, the stability of HM's base on  $\text{B}_2\text{O}_3$  constituent was insufficient. In this research, we excluded boron oxide in order to carry out simpler reactions. Fluoride oxide and lead oxide were used as inorganic components. To facilitate the possible exchange reaction, we carried out the study using thin films formed on glass substrates. The local temperature of the films' processing could substantially exceed the operating temperature of the glass substrate.

R. Saifutiyarov, Dr. O. Petrova, Dr. I. Taydakov, A. Akkuzina, A. Barkanov, M. Zykova, Dr. A. Lipatiev, Prof. V. Sigaev, Dr. R. Avetisov, V. Korshunov, Prof. I. Avetissov  
D. Mendeleev University of Chemical Technology of Russia  
P. N. Lebedev Physical Institute  
Russian Academy of Science  
Bauman Mscow State Technical University  
Moscow 125047, Russia  
E-mail: aich@rctu.ru

The ORCID identification number(s) for the author(s) of this article can be found under <https://doi.org/10.1002/pssa.201800647>.

DOI: 10.1002/pssa.201800647

Four types of structures on glass substrates were fabricated as research objects. The Type I structure consisted of 20 alternating layers of  $\text{Alq}_3$  (7.5 nm) and  $\text{PbO}$  (2 nm). The Type II structure consisted of 20 layers of  $\text{Alq}_3$  (7 nm) and  $\text{PbF}_2$  (2.1 nm). Structures (Type III and Type IV) were fabricated as heterophase mixtures of  $\text{Alq}_3$  (10 wt%) +  $\text{PbO}$  (Type III), and  $\text{Alq}_3$  (10 wt%) +  $\text{PbF}_2$  (Type IV) deposited simultaneously with 500 nm total thicknesses.

The as-deposited structures were transparent in the visible range of the spectrum, but they absorbed light in the 260–460 nm wavelength range, which is typical for  $\text{Alq}_3$  (Figure S1, Supporting Information). A joint analysis of PL spectra and optical luminescence microscopy (Figure 1 and 2) showed that Type I and Type III structures with an inorganic matrix based on  $\text{PbO}$  were characterized by a much higher homogeneity comparing to the Type II and Type IV structures with  $\text{PbF}_2$  inorganic constituent.

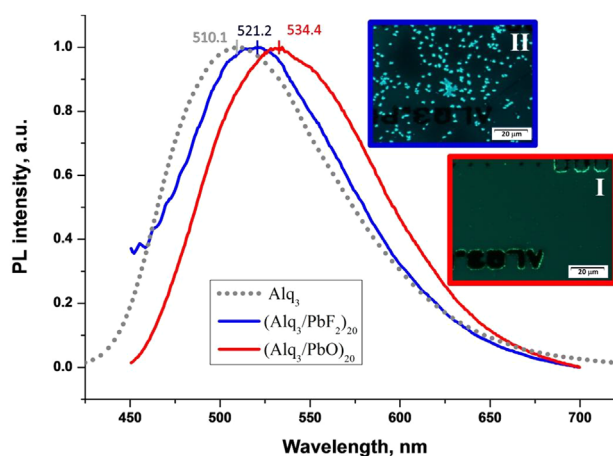


**Figure 1.** PL spectra and optical microscopy image under UV lighting of as-deposited Type I and Type II structures ( $\lambda_{\text{exc}} = 365$  nm) and pure  $\text{Alq}_3$  (100 nm) film.

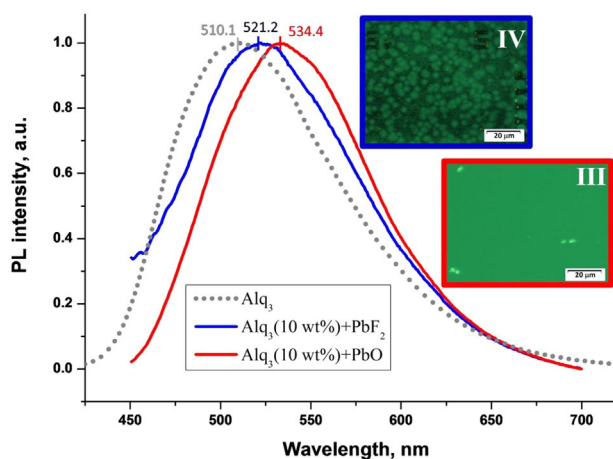


**Figure 2.** PL spectra and optical microscopy image under UV lighting of as-deposited Type III and Type IV structures ( $\lambda_{\text{exc}} = 365$  nm) and pure  $\text{Alq}_3$  (100 nm) film.

For all structures,  $\lambda_{\text{max}}^{\text{PL}}$  of the emission spectra was red-shifted comparing to that of the pure  $\text{Alq}_3$  films deposited at the same conditions (see Figure 1 and 3 dot line).

In the case of  $\text{PbO}$ -based structures, we observed the same value of  $\lambda_{\text{max}}^{\text{PL}} = 534.4$  nm for the both Type I and III structures. The PL spectra were broaden as it had been observed for bulk hybrid materials based on  $\text{Mq}_x$  ( $\text{M} = \text{Li}, \text{Rb}, \text{Sc}$ ) and 62(mol%)  $\text{PbO}$ -26(mol%)  $\text{B}_2\text{O}_3$ -12(mol%)  $\text{SiO}_2$  glass matrix.<sup>[16]</sup>

According to the experiments on fs-laser irradiation of polymers,<sup>[17]</sup> it was shown that specific bond was broken according to the smallest bonding strength about 50–80 mJ  $\text{cm}^{-2}$ . The threshold pulse energy was well correlated with the bond energy. Analysis of laser ablation of the fabricated structures (Figure 4) showed that in the case of  $\text{PbF}_2 + \text{Alq}_3$  (Type IV) structure for a single shot the threshold pulse energy was  $\approx 11$  nJ, while for  $\text{PbO} + \text{Alq}_3$  (Type III) structure it was close to  $\approx 2$  nJ (Figure 5, see insertion). In general, this result correlated with the energy bonds in inorganic matrices: the energy of  $\text{Pb}-\text{F}$  bond in  $\text{PbF}_2$  is about 330 kJ  $\text{mol}^{-1}$ <sup>[18]</sup> while  $\text{Pb}-\text{O}$  bond is as strong as 209 kJ  $\text{mol}^{-1}$ .<sup>[18]</sup>

Actually, the observed some difference in the threshold energies when compared with the bonds' energies as well as non-linear dependence of  $S_{\text{dot}} = f(\lg E)$  (Figure 5) could be explained by the fact that the fabricated heterophase structures could not be analyzed as single phase structures.<sup>[19,20]</sup> The nature of bonds in these heterophase structures could be subjected of the exchange reaction between ions of inorganic and organic constituents, and the reaction conversion during thin film fabrication could be far from 1. So, a part of laser energy during the ablation processing could be spent on the destruction of chemical bonds of the every constituent of the heterophase film both organic and inorganic. While another smaller part of the energy could spent on overcoming activation barriers of the chemical exchange reactions.

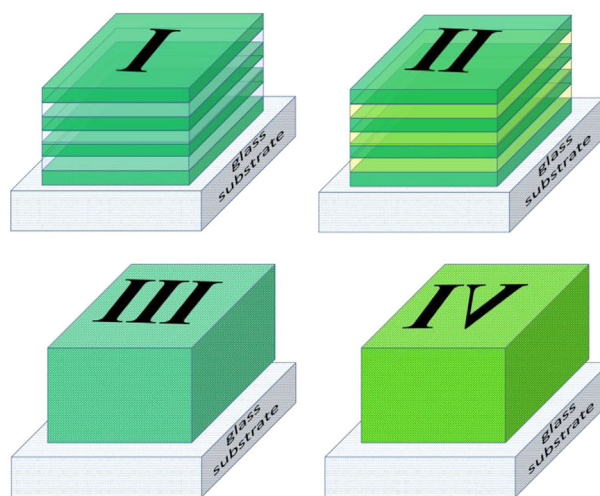


**Figure 3.** Topology of thin film structures based on  $\text{Alq}_3$ ,  $\text{PbO}$  and  $\text{PbF}_2$  on glass substrates (RMS = 2.5 nm): Type I –  $(\text{Alq}_3/\text{PbO})_{20}$  (190 nm); Type II –  $(\text{Alq}_3/\text{PbF}_2)_{20}$  (182 nm); Type III –  $\text{Alq}_3$  (10 wt%) +  $\text{PbO}$  (500 nm); Type IV –  $\text{Alq}_3$  (10 wt%) +  $\text{PbF}_2$  (500 nm).

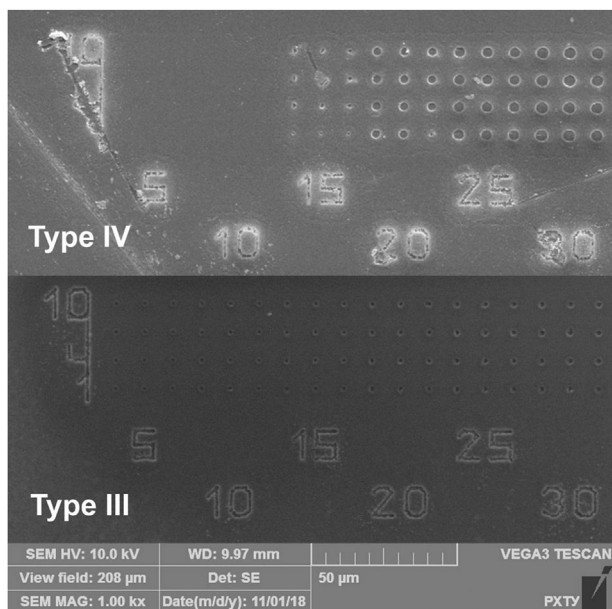
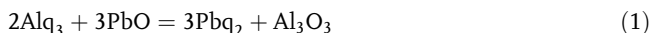


**Figure 4.** SEM images of Type IV and Type III structures laser irradiated by 1, 4, 7, and 10 pulses with pulse energy of 5–30 nJ and pulse repetition rate of 100 kHz.



We assume that optimizing of the conditions of laser exposure of the thin films Type III and Type IV will make it possible the full conversion of the exchange reaction (1, 2).

At higher intensities of laser radiation, the thermal decomposition of organic ligand has occurred, as indicated by

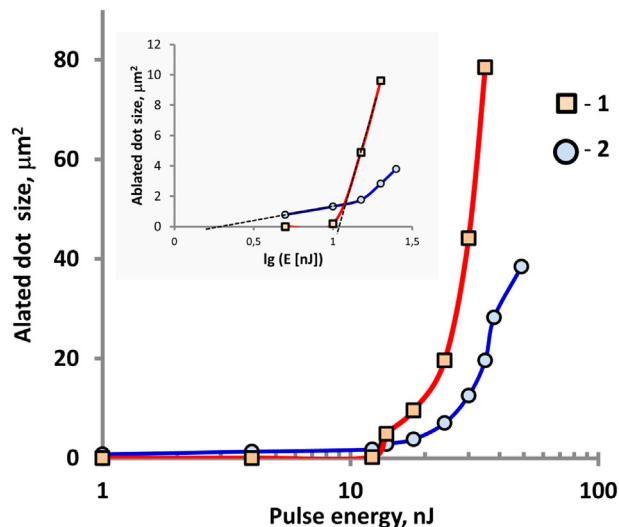


**Figure 5.** The ablated dot size vs fs-laser pulse energy for Type IV (1) and Type III (2) structures. The insertion shows the threshold energies determination. The dot diameter was defined as a recognized surface damage cross-section in SEM images.

the regions where no PL was observed (Figure S3, Supporting Information). When the laser pulse energy exceeded 40 nJ we observed the full destruction of the thin film structure due to its evaporation (Figure S4, Supporting Information). The same result has been achieved for the Type III structure (Figure S5–S7, Supporting Information).

The luminescent dots obtained at low radiation doses in the PbO-based Type I and Type III structure (Figure 6 and 7) were of particular interest. In the case of the Type I structure the dots were formed not regular in the area of low radiation. We explained it by possible inhomogenities in a thin film with 190 nm thickness whereas the Rayleigh length of focused laser beam is about 3 µm.

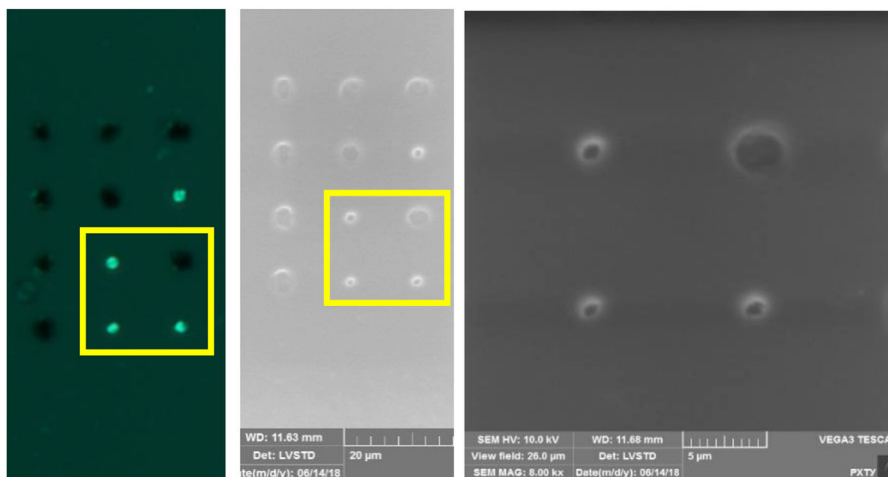


**Figure 6.** Optical microscopy of the Type I structure under UV lighting (left) and SEM images (center, right) of luminescent (small) and non-luminescent dots formed by laser irradiation with 10 or 100 pulses per a dot, pulse energy of 20 nJ and 100 kHz repetition rate and (the full array of dots is presented in Figure S2, Supporting Information).

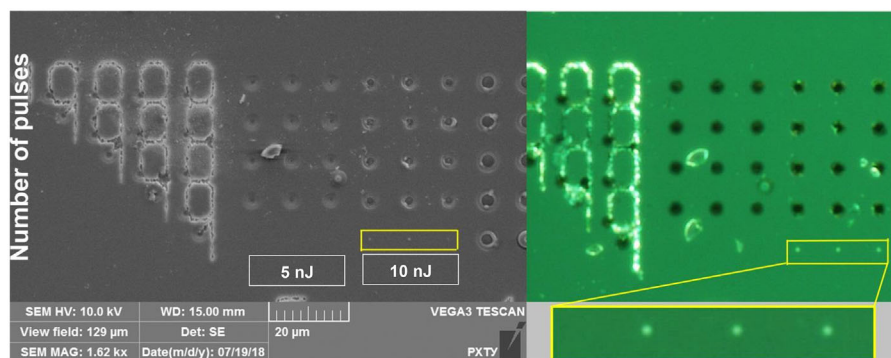


**Figure 7.** SEM image (left) and optical microscopy photo under UV lighting (right) of the Type III structure formed by fs-laser pulses with energy of 5–10 nJ.

Pulse energy of 10 nJ and only 1 pulse per dot were enough to conduct the exchange reaction and keep the film structure (Figure 5 and 8). For PbO-based structures, it was the best result in the range of the investigated laser exposure conditions.

Type II and Type IV structures containing PbF<sub>2</sub> as an inorganic matrix differed significantly from Type I and Type III (Figure 9, Figure S8 and S9, Supporting Information).

The as-prepared Type II had an inhomogeneous morphology and pronounced regions (1–2 μm) with increased PL (Figure S8, Supporting Information). So, the Type II structure was found ineligible for the further laser irradiation experiments.

The Type IV structure was also inhomogeneous. One could observe in epifluorescence microscopy images regular spheres of 3–5 μm in diameter (Figure 9). These spheres were located inside the film because SEM image demonstrated a smooth homogeneous surface (see Figure 9). Thus, we found the Type III and Type IV structures suitable for laser irradiation experiments.

The observed changing of the luminescence color of the PbF<sub>2</sub>-based structure in the form of bright dots (Figure S8, Supporting Information) can be explained as follows. It is known that cubic β-PbF<sub>2</sub> could dissolve dopants and form phosphors while α-PbF<sub>2</sub> due to cell structure restrictions does not appear as a luminescent matrix.<sup>[21,22]</sup> According to the study of HM (Alq<sub>3</sub>/PbF<sub>2</sub>/B<sub>2</sub>O<sub>3</sub>) an exchange reaction between Alq<sub>3</sub> and PbF<sub>2</sub> was

proceeded, in which the [Pb(q)F]<sub>2</sub> complex was presumably formed.<sup>[11]</sup> The similar complexes [Pb(q)I]<sub>2</sub> had been described by Najafi et al.<sup>[23]</sup> The PL spectrum of the complex is broadening comparing to that of Alq<sub>3</sub> (Figure 10).

Based on PL color we can suppose that the [Pb(q)F]<sub>2</sub> complexes are responsible for the bright luminescence. These complexes could form as a result of the spontaneous proceeding of the exchange reaction between Alq<sub>3</sub> and β-PbF<sub>2</sub> during the multilayer structure fabrication.

The similar process could proceed while the Type IV structure was fabricated. However, in this case the spheres of HM contained partially [Pb(q)F]<sub>2</sub> complexes and unreacted initial constituents were formed.

The laser irradiation of the Type IV structure showed that at comparatively low pulse energy of 10 nJ by applying just 1 or 10 pulses per dot we can form regular dots with bright luminescence (Figure 10). It should be noted that the dots were formed in any place of the film structure both in the areas of the bright spheres and in dark places. It could be explained by the initiation of the exchange reaction proceeding under the femtosecond laser impact.

Increasing the pulse energy to 25 nJ resulted in the damage of the thin film structure (Figure 11). An impact of 1 pulse per dot allowed keeping the film structure, but according to the SEM analysis, a small hole in the film was formed. When we increased the number of pulses to 10 and more, the film structure was strongly modified. One could observe swollen areas which in some cases split off from the film surface and formed circle holes.

Taking into account these results, Type III structure was irradiated by small number of pulses. There is practically no destruction of the film at low irradiation energies, but we observed the change in the luminescence color.

PL kinetics was measured at a point in the area not exposed to laser processing point 1 in Figure 12. We did not observe any difference in the not-exposed dot and the dot irradiated by 1 pulse with 5 nJ energy. For these both dots, the PL decay kinetics has a biexponential form of relaxation with characteristic times of the order of  $\tau_1 = 2$  ns and  $\tau_2 = 5$  ns (Figure 13, curve 1). In the laser-induced region (Figure 12, point 2), the luminescence kinetics has a three-exponential form with characteristic times on the order of  $\tau_1 = 1$  ns,  $\tau_2 = 2.1$  ns, and  $\tau_3 = 3.6$  ns (Figure 13, curve 2).

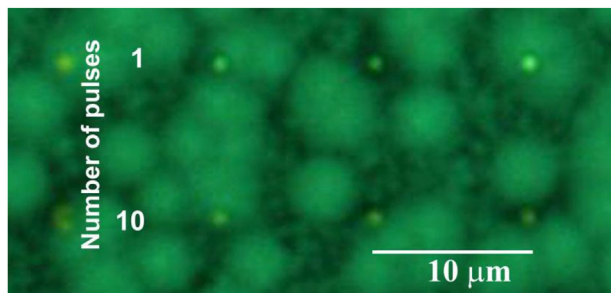


**Figure 8.** Optical microscopy images under UV lighting of arrays of dots in the Type IV structure formed under action of laser pulses with energy of 10 nJ.



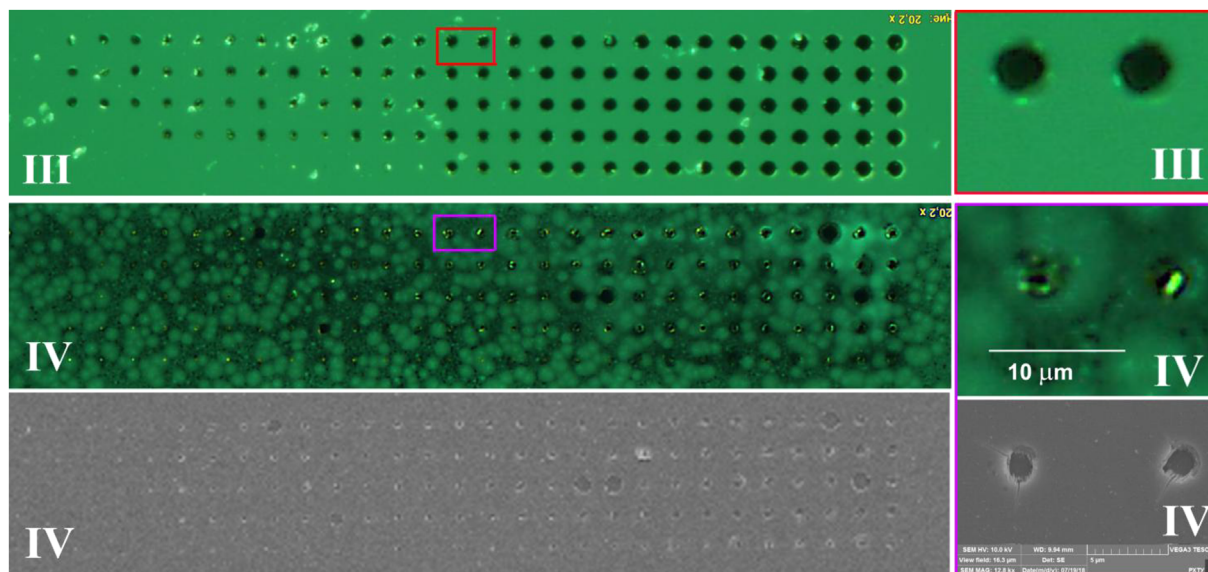


**Figure 9.** Optical microscopy images under UV lighting ( $20\times$ ) of arrays of dots in the Type III and Type IV structures laser irradiated and magnified views of dots (right column) formed by pulses with energy of 60 nJ.

The observed difference in PL decay kinetics proved the suggestion that the fs-laser irradiation resulted in the formation another phosphor towards the initial  $\text{Alq}_3$ .

## 2. Conclusions

The possibility to form the regular 2D structure of luminescent hybrid materials in thin films has been demonstrated. It was established that for the organic–inorganic hybrid material based on tris(8-hydroxyquinoline)aluminum as organic constituent and  $\text{PbO}$  or  $\text{PbF}_2$  as inorganic constituents a new luminescent HM could be formed under the action of a focused femtosecond laser beam. The exchange solid phase reaction is efficiently stimulated at the laser pulse energy starting from 10 nJ (laser pulse fluence  $1270 \text{ mJ cm}^{-2}$ ). To carry out the reaction and preserve the structure of a thin film, only 1–4 pulses are required. The higher radiation doses resulted to the destruction

of the HM film. Localization of the reaction region is determined by the focused laser beam waist ( $\approx 1 \mu\text{m}$  in diameter).

## 3. Experimental Section

**$\text{Alq}_3$  Synthesis and Purification:** Organometallic coordination compound was prepared in one step according to the modified procedure. 3.5 g of 8-hydroxyquinolinol (sublimated grade 99.9991 wt%) was dissolved in 50 ml of isopropanol (99.9953 wt%) at continuous stirring in 100 ml Teflon beaker at  $25 \pm 1^\circ\text{C}$ .  $\text{Al}(\text{NO}_3)_3$  (99.989 wt%) in 0.8 equimolar amount was added into solution at continuous stirring during 1 h.  $\text{NH}_4\text{OH}$  (99.9960 wt %) was added dropwise to  $\text{pH} = 10$  and yellow solid precipitated. The solid was filtered using grass porous filter (GF/F Whatman) and washed by two portions of n-hexane (50 ml, 99.9943 wt%). 5 g of  $\text{Alq}_3$  was placed in a 100 ml Teflon beaker and n-hexane (30 ml) was poured into the beaker. The mixture was heated with constant stirring to boiling. The solution was cooled to RT and solid was precipitated. The precipitate was filtered off on a glass Schott filter and washed with two 10 ml n-hexane

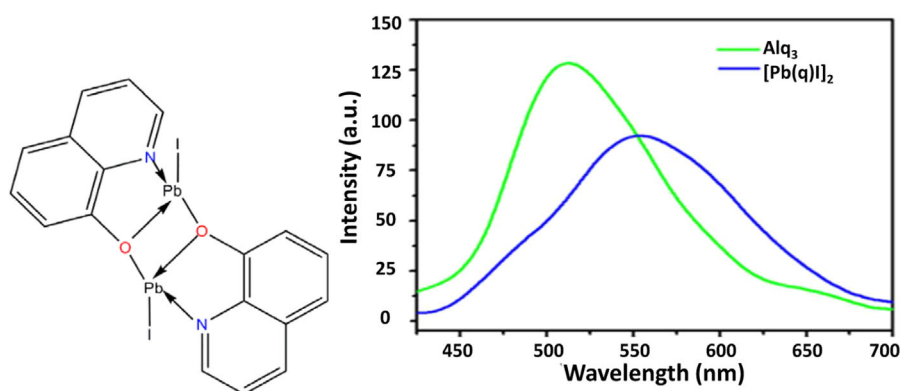


**Figure 10.** Photoluminescence spectra of powdered  $\text{Alq}_3$  and  $[\text{Pb}(\text{q})\text{I}]_2$  complexes.<sup>[15]</sup>

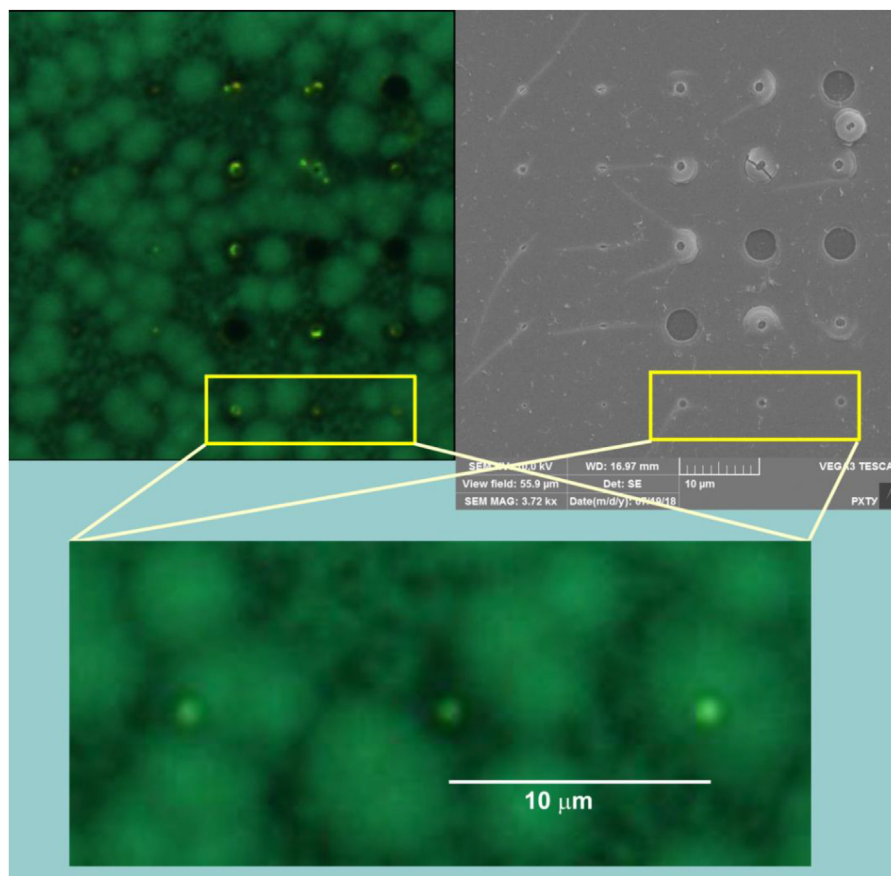


**Figure 11.** Optical microscopy images of arrays of dots in the Type IV structure formed by radiation power 25 nJ under UV lighting (top-left), SEM images (top-right), and magnified views (bottom).

portions. The final precipitate was dried for 6 h in a quartz glass reactor at 323 K under  $1 \times 10^{-4}$  Torr. Yield – 71% of yellow solid.

The obtained precipitates of  $\text{Alq}_3$  were purified by sublimation in dynamic vacuum ( $p = 10^{-7}$  Torr) using step-by-step heating (50 °C step to 250 °C), 30 min exposure at every step and 5 h processing at 250 °C.

*Thin Film Fabrication:* Multilayers thin film structures have been fabricated by vacuum thermal sputtering ( $< 10^{-5}$  Pa) on a glass substrate (RMS = 2.5 nm).  $\beta\text{-PbO}$  (99.99 wt%) and  $\text{PbF}_2$  (99.98 wt%) were used as inorganic compounds. Quartz glass container with W-wire heater was used for  $\text{Alq}_3$  sputtering  $\text{PbO}$  and  $\text{PbF}_2$  were sputtered from Mo-foil resistive

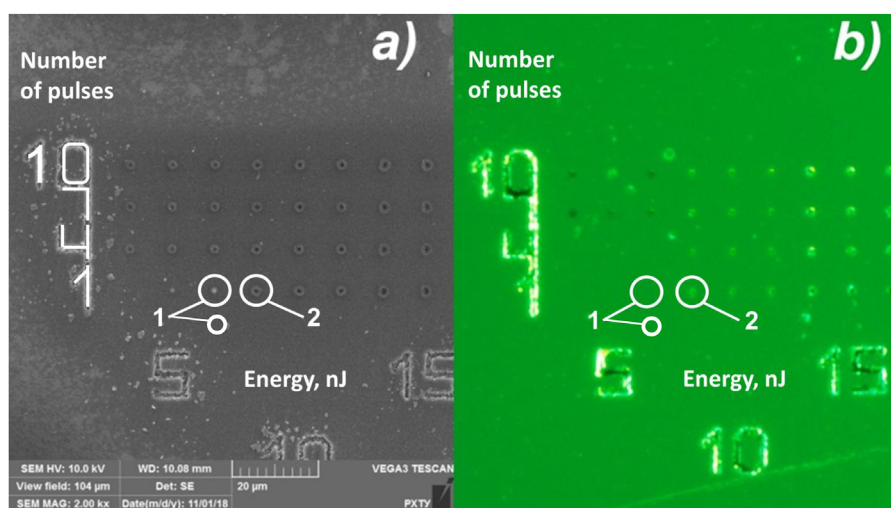


**Figure 12.** SEM and optical microscopy images under UV lighting of Type III structure. 1 and 2 areas were used for analysis of PL decay kinetics.

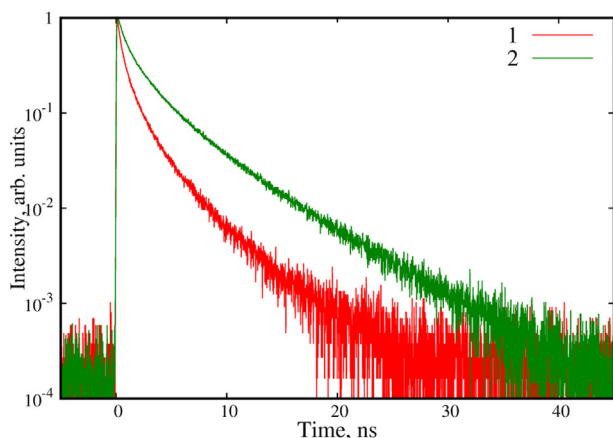


**Figure 13.** Kinetics of luminescence at the points indicated in Figure 11 for Type III structure: 1 – in the area not exposed by the fs-laser, and 2 – the area after laser irradiation by 1 pulse and 10 nJ.

heater. The deposition rates of  $0.015 \text{ nm} \times \text{s}^{-1}$  for each component lets fabricate the structure both with a layer-by-layer topology or with a simultaneous deposition of two components, i.e.,  $\text{Al}_3$  and  $\text{PbO}$  ( $\text{PbF}_2$ ).

**Laser Irradiation:** Femtosecond laser Pharos SP (wavelength 1030 nm) was used for thin film modification. The laser was tuned to a minimal pulse duration of 180 fs, pulse repetition rate of 100 kHz. The laser beam was focused at the thin film by the objective lens Olympus LCPLN IR 100 $\times$  (0.85 NA objective). The sample was translated in the plane perpendicular to the focused laser beam by means of motorized air-bearing stage Aerotech ABL1000. The pulse energy measured after focusing objective and number of deposited pulses were varied from 5 to 50 nJ and from 1 to  $10^4$ , respectively. For each pulse energy and number of pulses, three dots were written in thin films with different laser beam polarization of 0, 45, and 90 degrees. The spot diameter was  $\approx 1 \mu\text{m}$  which results to the laser fluent of  $640 \text{ mJ cm}^{-2}$  at 1 pulse and 5 nJ power. The observation of the laser modified dot arrays was performed by an Olympus BX51 luminescence microscope. The fluorescence images were obtained using Olympus U-MNV2 filter cube which provides excitation in 400–410 nm range and emission registration from 455 nm. Birefringence of laser-written dots was analyzed by Abrio micro-birefringence system installed on polarizing optical microscope Olympus BX61.

**Scanning Electron Microscopy (SEM):** SEM images of the thin film samples were obtained using a VEGA-3 LMU instrument (TESCAN Corp.) in secondary electron (SE) mode with 10 kV accelerating voltage. Taking into consideration the dielectric nature of the samples 1.5–2 nm Au film was deposited on the samples.

**Photoluminescence:** Emission spectra of the structures were measured in backscattering mode using an QE65000 spectrometer (Ocean Optics, Inc., USA) equipped by 3 mm fiber optic cable with a splitter for input of the exciting radiation from diode laser (365 nm) and output the emission (PL) radiation in the 400–800 nm wavelength region. The spectra were irradiated by an OriginPro 8 SR4 software.

Luminescence decays were measured using a PicoQuant MicroTime 200 system implementing time-correlated single photon counting (TCSPC) technique. The sample was placed onto the microscope stage of an Olympus microscope. The excitation laser radiation and the sample luminescence were collected via an UPlanSApo 100 $\times$  objective. PDL 828 semiconductor-pulsed laser light source emitting at 376 nm with 50 ps pulse duration and 100 kHz repetition rate was used for optical excitation. Picosecond decay time resolution was provided by a  $\tau$ -SPAD avalanche photon detector coupled to a PicoQuant PicoHarp 300 time-correlated single photon counting system. Spectral band with maximum at 530 nm was selected by interference band-pass filter (Chroma, USA) with a bandwidth of 10 nm.

## Supporting Information

Supporting Information is available from the Wiley Online Library or from the author.

## Acknowledgements

The research was supported by the Russian Science Foundation by grants 14-13-01074II (luminescent hybrid materials) and Russian Foundation for Basic Research 16-32-60035 (high pure  $\text{Al}_3$  synthesis), 16-03-00541 (laser-induced transformation in solids).

## Conflict of Interest

The authors declare no conflict of interest.

## Keywords

femtosecond lasers, hybrid materials, luminescence, organometallic phosphor

Received: August 14, 2018

Revised: November 23, 2018

Published online:

- [1] D. Zhao, W. Qin, C. Wu, J. Zhang, G. Qin, H. Lin, *J. Rare Earths* **2004**, 22, 49.
- [2] C. Huang, T. Sun, W. Tian, B. Zhao, *J. Rare Earths* **2006**, 24, 134.
- [3] X. Hao, X. Fan, M. Wang, *Thin Solid Films* **1999**, 353, 223.
- [4] D. Bersani, P. P. Lottici, M. Casalboni, P. Proposito, *Mater. Lett.* **2001**, 51, 208.
- [5] L. D. Carlos, *Electrochim. Acta* **2000**, 45, 1555.
- [6] X. Fan, Z. Wang, M. Wang, *J. Lumin.* **2002**, 99, 247.
- [7] S. Li, J. Lu, M. Wei, D. G. Evans, X. Duan, *Adv. Funct. Mater.* **2010**, 20, 2848.
- [8] T. Watanabe, N. Doki, M. Yokota, K. Shimizu, in *Materials of the 13th Asia Pacific Confederation of Chemical Engineering Congress (APCCChE 2010)* (Taipei, 2010).
- [9] I. Pritula, V. Gayvoronsky, Yu. Gromov, M. Kopylovsky, M. Kolybaeva, V. Puzikov, A. Kosinova, Yu. Savvin, Yu. Velikhov, A. Levchenko, *J. Opt. Commun* **2009**, 282, 1141.
- [10] O. B. Petrova, R. I. Avetisov, A. V. Khomyakov, R. R. Saifutyarov, A. A. Akkuzina, E. N. Mozhevitina, A. V. Zhukov, I. Ch. Avetissov, *Eur. J. Inorg. Chem.* **2015**, 7, 1269.
- [11] O. B. Petrova, M. O. Anurova, A. A. Akkuzina, R. R. Saifutyarov, E. V. Ermolaeva, R. I. Avetisov, A. V. Khomyakov, I. V. Taydakov, I. Ch. Avetissov, *Opt. Mat.* **2017**, 69, 141.
- [12] O. Petrova, I. Taydakov, M. Anurova, A. Akkuzina, R. Avetisov, A. Khomyakov, E. Mozhevitina, I. Avetissov, *J. Non-Crystal. Solids* **2015**, 429, 213.
- [13] I. Taydakov, M. Anurova, A. Akkuzina, R. Avetisov, A. Khomyakov, I. Avetissov, O. Petrova, *Period. Polytech. Chem. Eng.* **2016**, 60, 152.
- [14] R. R. Saifutyarov, A. V. Khomyakov, A. A. Akkuzina, R. I. Avetisov, O. B. Petrova, I. Kh. Avetisov, S. V. Kravchenko, *Opt. Spectrosc.* **2015**, 119, 84.
- [15] S. S. Fedotov, S. V. Lotarev, A. S. Lipatiev, M. Beresna, A. Cerkaskaite, V. N. Sigaev, P. G. Kazansky, *Appl. Phys. Lett.* **2016**, 108, 071905.

- [16] O. Petrova, R. Avetisov, A. Akkuzina, M. Anurova, E. Mozhevitina, A. Khomyakov, I. Taydakov, I. Avetissov, *IOP Conf. Ser.: Mater. Sci. Eng.* **2017**, 225, 012083.
- [17] L. Wang, X.-W. Cao, C. Lv, H. Xia, W.-J. Tian, Q.-D. Chen, S. Juodkazis, H.-B. Sun, *IEEE J. Quantum Electron.* **2018**, 54, 9200207.
- [18] D. R. Lide (Ed.), *CRC Handbook of Chemistry and Physics*, CRC Press, Boca Raton **1990**.
- [19] X.-W. Cao, Q.-D. Chen, H. Fan, L. Zhang, S. Juodkazis, H.-B. Sun, *Nanomaterials* **2018**, 8, 287.
- [20] X. Wang, A. Kuchmizhak, D. Storozhenko, S. V. Makarov, S. Juodkazis, *ACS Appl. Mater. Interfaces* **2018**, 10, 1422.
- [21] T. S. Sevostjanova, A. V. Khomyakov, M. N. Mayakova, V. V. Voronov, O. B. Petrova, *Opt. Spectrosc.* **2017**, 123, 733.
- [22] J. Pisarska, T. Goryczka, W. A. Pisarski, *Solid State Phenom.* **2007**, 130, 263.
- [23] E. Najafia, M. V. Amini, E. Mohajerani, M. Janghour, H. Razavi, H. Khavasi, *Inorg. Chim. Acta.* **2013**, 399, 119.